



**Experimental demonstration of throughput advantage of a static Fourier Transform spectrometer (HES 2003) when performing Transmission and stand-off Raman observations.**

**M. Foster, M. Zentile, and J. Storey**

## 1. Executive summary

This report describes the first demonstration of a new spectrometer that can be coupled to a 3 mm diameter optical fibre without the use of a slit and achieve  $< 4 \text{ cm}^{-1}$  resolution. The system is based on a static Fourier transform concept [AD1]. The instrument has been tested by making transmission Raman observations with the light coupled to the spectrometer via a range of fibres of different apertures. No loss of resolution was observed, while light increased as a function of the fibre collecting area. The system was also tested in a standoff Raman configuration where similar gains were observed. The total throughput gain is estimated as being  $> 500$  times that of a traditional dispersive system.

## 2. Introduction

### 2.1. Raman observations

In recent years Raman measurement has become an increasingly prominent tool for a variety of applications including: Quality assurance (QA) measurements in the process sector, detection of explosive and counterfeit drugs by the security sectors and providing on line measurements in the manufacture of pharmaceuticals. Classic Raman observations are made in a backscatter configuration with the target 10 – 20 mm from the instrument collection optics. This approach is widely used by hand held devices in the field.

However, this approach is not ideal for many industrial applications, particularly when a bulk measurement of the sample is required or if the sample is heterogeneous in nature. In recent years transmission Raman observations have re-emerged [AD2] as an ideal technique for many QA applications. This method allows Raman photons to be observed from the entire sample, rather than a single, localised point on the surface. This approach does, however, possess several challenges to the Raman spectrometer.

1. The signal strength is typically lower compared with a backscatter arrangement
2. Light exiting the sample comes from a significantly increased Area (A)  $\times$  Solid angle ( $\Omega$ ) product.

It is the latter of these two issues that must be overcome by the spectrometer design. Any spectrometer for a given resolution can only accept light from the A  $\Omega$  product, or étendue. In a Czerny Turner configuration this is typically controlled by the slit width [AD3]. A static Fourier transform spectrometer, such as ISI's HES range [AD4], can deliver  $> 100$  times increase in the total throughput when compared to a dispersive system, with a potential increase in excess of a factor of 500.

The étendue problem is also present when performing stand-off Raman observations at distances beyond 60 mm. This can limit the use of Raman systems to study processes in challenging environments such as high temperature process vessels.

In this technical note we will explore the étendue advantage provided by static Fourier transform spectrometers in detail. A new device has been developed based on a spatial heterodyne spectrometer [AD1], [AD5], which can accept fibre inputs from 50 µm core diameter up to 3 mm. This maximises the advantage of the system, potentially providing a throughput gain of over 1000 times greater than a Czerny Turner instrument of similar resolution.

### 3. The Raman Spectrometer

The specifications for the developed Raman spectrometer are given in Table 1. The spectrometer is fibre coupled, either via a fibre SMA connector or by a bespoke design to accommodate a >3 mm core fibre. The collimating and imaging lens both have a working aperture of 50 mm and a focal length of 80 mm and 100 mm respectively. To ensure all the light was captured an acylindrical lens is mounted ahead of the detector.

**Table 1** Specifications of spectrometer

| Parameter                                     | Value                                       | Notes               |
|---|---|---------------------|
| Laser   |   |                     |
| Operating wavelength                          | 785 nm                                      |                     |
| Power   | 500 mW                                      | Laser fibre coupled |
| Gratings area                                 | 2 × (52 × 52 mm)                            |                     |
| Lines per mm                                  | 60  |                     |
| Working aperture                              | 34.4 mm                                     |                     |
| Detector                                      | Andor IVAC                                  |                     |
| Pixels  | 1650 × 200                                  |                     |
| Pitch   | 16 µm                                       |                     |
| Resolution                                    | 3.1 cm <sup>-1</sup>                        | Per pixel           |
| Spectral range                                | 50 cm <sup>-1</sup> – 2500 cm <sup>-1</sup> |                     |
| Maximum theoretical acceptance fibre aperture | 3.4 mm                                      | Diameter            |
| Fibre NA                                      | 0.22  |                     |

The detector used was a cooled IVAC CCD provided by Andor was used as the detector, as with previous HES2000 models. The detector was cooled to – 60 °C and has 1650× 200 pixels. The illumination source was a 785 nm diode laser with a output laser power is 500 mW, (however some light is lost via the fibre coupling), the laser bandwidth of < 100 pm. Two long pass filters are used to suppress the Rayleigh scattering and a narrow bandwidth filter ( FWHM = 4 nm) was mounted immediately after the laser output fibre to suppress any contaminant wavelengths.

The range of ‘receive’ fibres used for the test program is given in Table 2. The fibre lengths were 2 m and were terminated with SMA connectors, with the exception of the 3 mm bundle, which was terminated with a custom ferrule. The 2 mm and 3 mm diameter fibres were both constructed from a bundle of 550  $\mu\text{m}$  core fibres.

**Table 2** *List of Fibres*

| Fibre Diameter | Fibre Na | Type / Notes   |
|----------------|----------|--|
| 3 mm           | 0.22     | Bundle 17 fibres with 0.55 mm core diameter NA of 0.22 |
| 2 mm           | 0.22     | Bundle 7 fibres with 0.55 mm core diameter NA of 0.22  |
| 1 mm           | 0.39     | Multimode  |
| 0.91 mm        | 0.22     | Multimode  |
| 0.6 mm         | 0.22     | Multimode  |
| 0.55 mm        | 0.22     | Multimode  |
| 0.4 mm         | 0.39     | Multimode  |
| 0.2 mm         | 0.39     | Multimode  |
| 0.05 mm        | 0.22     | Multimode  |

The measurements were made against a 3 mm thick paracetamol tablet. The tablet was illuminated with 1 mm diameter laser spot at 785 nm and observed in a Transmission Raman configuration. By using a transmission Raman setup, it is guaranteed that the étendue of the target light will be large, with light coming from a significant fraction of the tablet surface area and acting as a Lambertian scatterer. The light capture assembly used two 50 mm focal length lenses, set to capture the same sized area on the tablet as the fibre core (so magnification = 1), with an NA of  $\sim 0.22$ . This ensured that when the higher NA fibres were used, the higher modes were not excited, so the light that exited the fibre had an NA of  $\sim 0.22$ .

### 3.1. Quality of Diffraction Gratings

Given the large illuminated aperture at the diffraction gratings, issues with the underlying plate flatness must be examined. This is illustrated in Figure 1, where the plates are held under tension and the resulting fringe pattern from the laser is examined, with the system tuned just off a Littrow configuration. The shape of the fringes indicate that the plate flatness is worse than  $\lambda/2$  (a red line has been added to indicate the path of a perfect fringe), therefore if the fringes are compressed by a cylindrical lens, resolution would be lost.

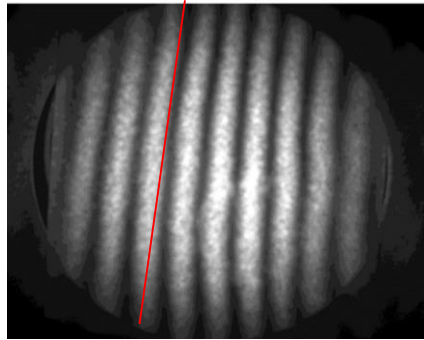


**Figure 1** Underlying Fizeau Fringe pattern for HES spectrometer but with plates placed under tension

Once the tension is released the relative distortion in the fringes is reduced (Figure 2), thus allowing the fringes to be compressed by the cylinder.

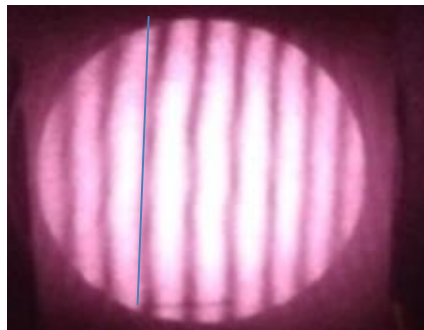


**Figure 2** Underlying Fizeau Fringe pattern for HES spectrometer with tension in the plates reduced.

This is a key step to ensuring the best resolution of the system can be achieved. It should be noted that in the Fizeau fringe configuration is the relative distance between the fringes that is critical. With the gratings correctly tuned, the final spectrometer is shown in Figure 3 with the 3 mm fibre ferrule mount installed.

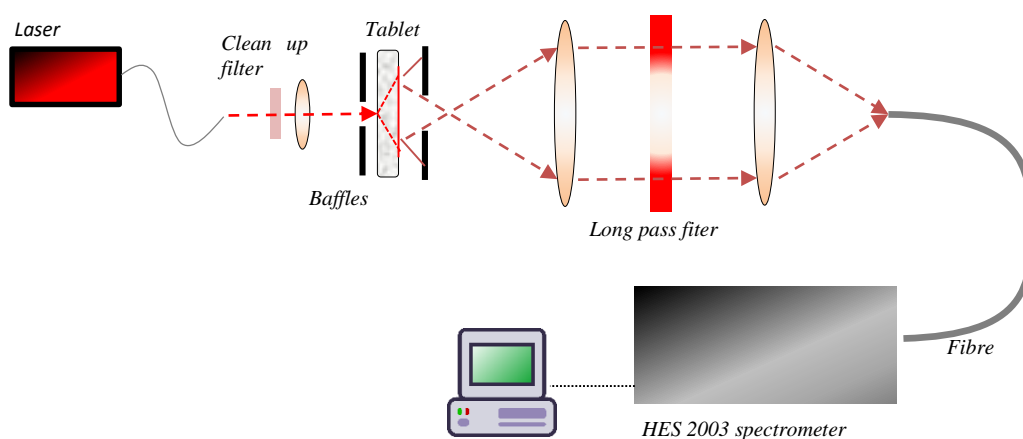


**Figure 3** HES 2003 spectrometer

## 4. Transmission Raman Experiments

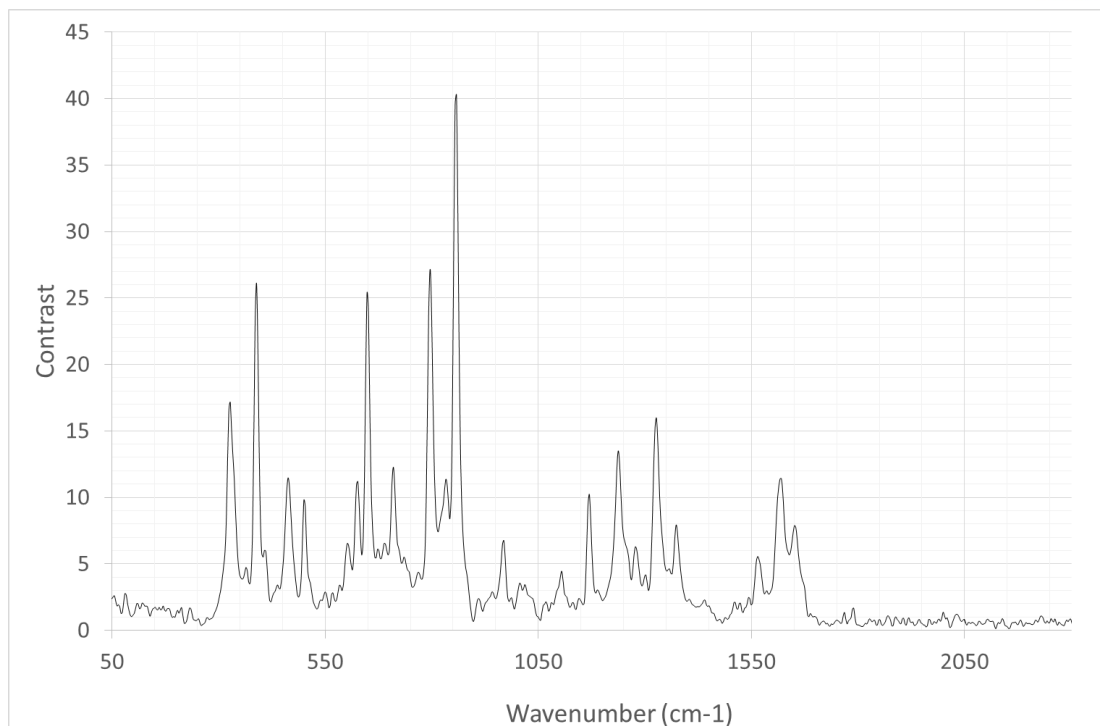
### 4.1. The baseline spectra

Figure 4 shows the setup for collecting the transmission Raman light and coupling it into the spectrometer. The fibre (bundle) was the only part replaced in each of the experiments. All tests were performed against the same 3 mm thick paracetamol tablet. The tablet had its outer coating removed in order to provide clean spectra, free of fluorescence.



**Figure 4** Transmission Raman configuration

To generate a base spectrum to which all other data sets could be compared, a spectrum was taken using a 2 mm fibre bundle with an integration time of 2.5 seconds, giving an average number of counts per pixels of 3970. The resulting spectrum is given in Figure 5. The data were apodised with a Hanning window before it was Fourier transformed. No other processing was performed. This ensured high signal to noise was achieved, whilst ensuring practical exposure lengths could be used to collect the same signal levels when using smaller core fibres. The detector dark count was negligible, however the read noise was measured as  $6 \text{ counts s}^{-1} \text{ pixel}^{-1}$ .



**Figure 5** Paracetamol spectra, light coupled via a 2 mm fibre bundle.

Additionally, a background count rate (of  $\sim 0.3 \text{ counts s}^{-1} \text{ pixel}^{-1}$ ) was also measured when the laser was turned off. This was due to an imperfect light seal with the system to accommodate the different fibre mounting mechanisms.

The fibre was systematically exchanged for each of the fibres given in Table 2, the exposure time adjusted to produce 3970 counts per pixel and the spectra recorded. A selection of these is given in Figure 6. It should be noted that both fibre bundles were arranged in a round to round configuration.

When using the 0.39 NA fibres care was taken to ensure the minimum number of bends to minimise the excitation of higher modes. This was confirmed by visual observation.

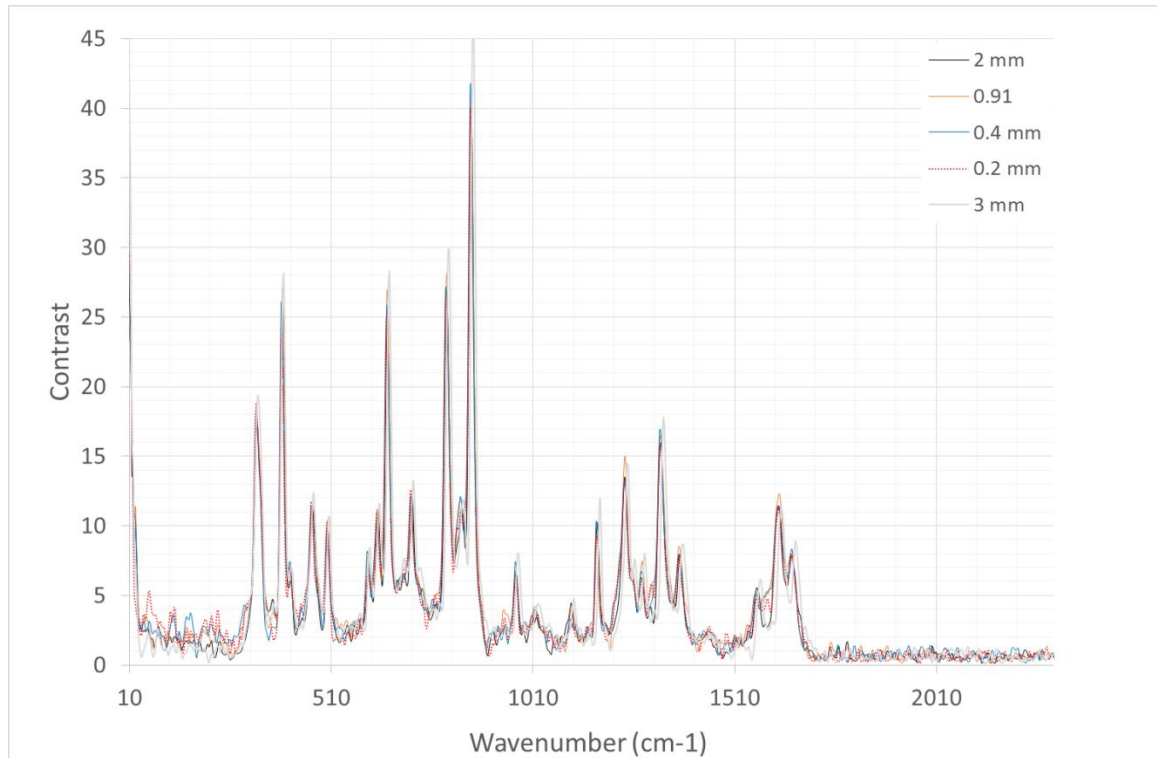


**Figure 6** Paracetamol Raman spectra measured in transmission, light is coupled by fibre of different diameters: Black Line= 2 mm fibre bundle; orange line = 0.91 multimode fibre; blue line = 0.4 mm multimode fibre; red dotted line = 0.2 mm multimode fibre; grey line = 3 mm fibre bundle.

The final fibre to be tested was the 3 mm fibre bundle. When using this fibre bundle the coupling assembly had to be adjusted to allow the 3 mm ferrule to be used. The resulting spectrum is given Figure 7. For comparison the spectra from the 1 mm diameter 0.39 NA fibre is also displayed. The required exposure time in this instance was 1.09 s. No loss of resolution was observed and the peaks around  $1630\text{ cm}^{-1}$  appear better resolved than when using the smaller fibres. This is due to the increased divergence of the light exiting the bundle illuminating more lines at the grating surface. There is also a small shift in the calibration when using the 3 mm aperture fibre. This was generated when the SMA connector was replaced by the 3 mm ferrule mount and the relative positions not being identical.

The resolving power of the system is given by

$$R = 2Dg$$

Where D is the diameter of beam being illuminated (34.4 mm in the case) and g is the number of lines per mm for the grating.



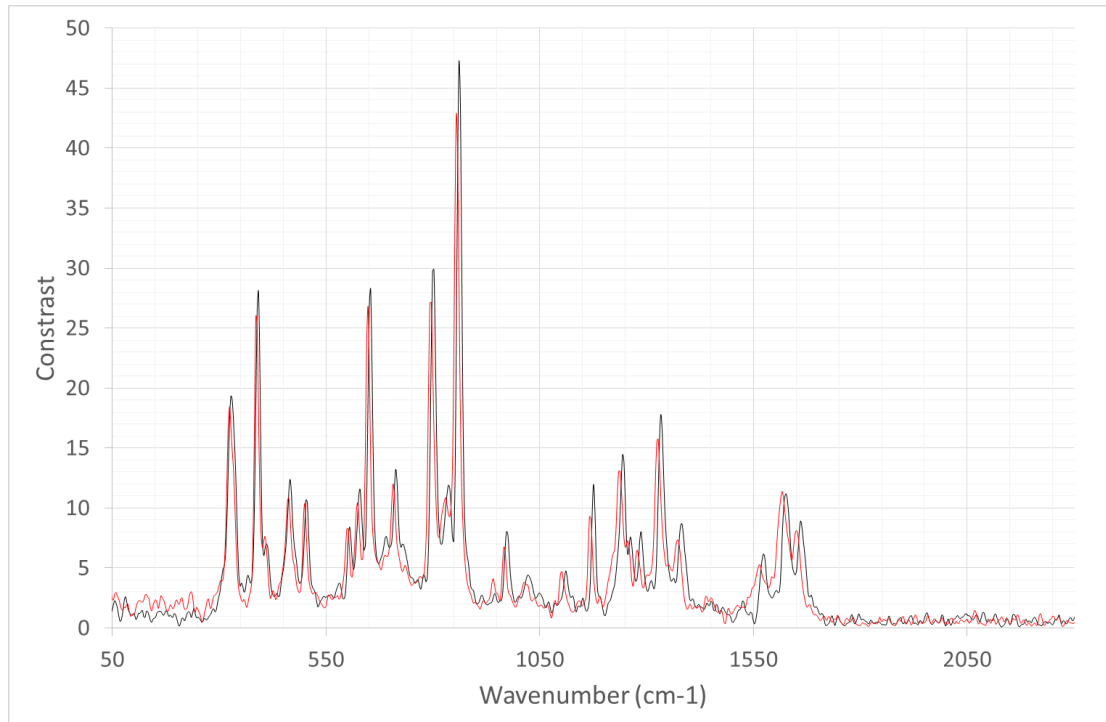


**Figure 7** Paracetamol spectra, light coupled via a 3 mm fibre bundle (Black line), light coupled via a 1 mm diameter fibre with a NA of 0.39 (red line)

This is a clear demonstration of the spectrometer's ability to resolve all the required features when using a 3 mm diameter fibre, ensuring that light would have been collected from the majority of the tablet's exit face.

## 4.2. Error sources

Assuming the surface of the tablet being examined is a perfect Lambertian scatterer with a diameter  $> 3$  mm and there are no other light sources, then the amount of the light collected will be proportional to the surface area of the fibre. As the fibres are changed then, for a given signal to noise ratio, the resolution should be unchanged as larger apertures are used. To confirm this a high signal photon level was chosen to which all measurements must be compared. This was set as being 3970 counts per pixel, or 2.5 s exposure time when using the 2 mm fibre bundle. The expected exposure time used for each of fibres to achieve this level was then calculated by taking the ratio of the area of the fibre to the active area of the 2mm fibre bundle. Due to the geometry of the fibre bundle some collecting area is lost for each of these 47 % (2 mm bundle) and 43 % (3 mm bundle).

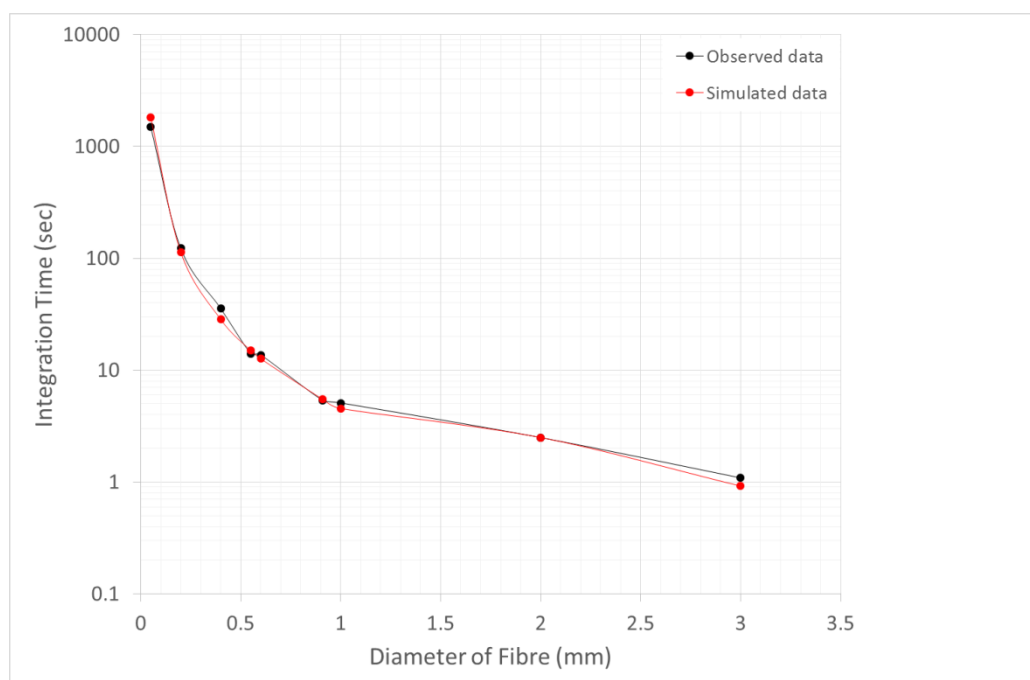
A number of errors sources were observed during the observations

- The laser power was noted to fluctuate on timescales of several minutes by up to 5 %
- The surrounding temperature of room effected the DC offset on the detector counts by up to 10 counts (nominal value was 490 counts per pixel)
- Background light sources were estimated as being 0.3 per second.

To minimise these effects all observations were repeated three times and the mean taken. For integration times below 10 s the standard deviation in the measurement was estimated as being 0.15 s. For measurements of 20-60 s this increased to ~0.5 s. When using the very small core fibres the background light source started to impact the results. This is particularly true when the 50  $\mu\text{m}$  diameter fibre was used. The standard deviation in this case increased to 25 s (observed integration time was 1500 s).

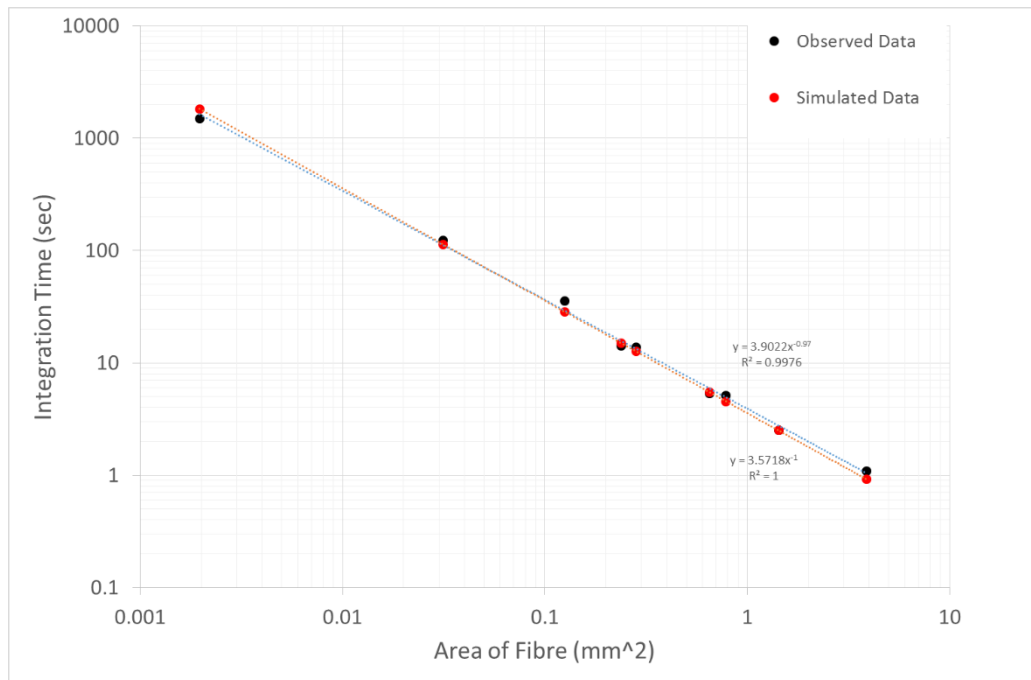
### 4.3. Throughput results

Figure 8 shows the required integration time to observe 3970 counts per pixel for each of the fibres as a function of their diameter. The black line represents the observed results and the red line shows the calculated levels.



**Figure 8** Required integration time to observe 3970 counts per pixel as a function of fibre diameter (Red line = simulated data; Black line = Observed data)

The observed data is in a good agreement with the calculated response across the range. This is further illustrated within Figure 9, which shows the exposure time plotted as a function of area displayed in a log/log plot. It should be noted that the 400  $\mu\text{m}$  fibre consistently demonstrated slightly poorer performance than expected. After inspection it was determined this was due to slight damage to one of the end faces of the fibre, resulting in increased losses. The overall consistency of the results was excellent, with the observed power coefficient of -0.97 compared to the target value of -1.



**Figure 9** Required integration time to observe 3970 counts per pixel as a function of fibre area (Red line = simulated data; Black line = Observed data)

This demonstrates both that when in a transmission Raman configuration the tablet does act as a Lambertian scatterer with an aperture of  $> 3 \text{ mm}$ , and that the spectrometers étendue acceptance is at least  $7.065 \text{ mm}^2$  with a NA of 0.22 to maintain a resolution of  $4\text{cm}^{-1}$ . It should be noted that the actual collection area is  $4.027 \text{ mm}^2$  due to the gaps in the fibre bundle arrangement. However when determining the acceptance area, it the total synthetic area that is key criteria.

## 5. Standoff Raman observations

The setup of the experiment was adjusted into a standoff backscatter configuration (Figure 10). The tablet was located approximately 70 mm from a mono-axial LIDAR arrangement. The laser spot at the tablet was estimated as being  $\sim 2.5 \text{ mm}$  in diameter, and the telescope focussed at the surface of the tablet. In this arrangement the scatter from the surface of the tablet is expected to be broadly Lambertian in nature from the 2.5 mm diameter ( $\sim 5 \text{ mm}^2$  area). However, there may be some Gaussian bias due to the intensity profile of the laser. Also, in this arrangement, the signal strength is expected to be higher than in the transmission configuration.

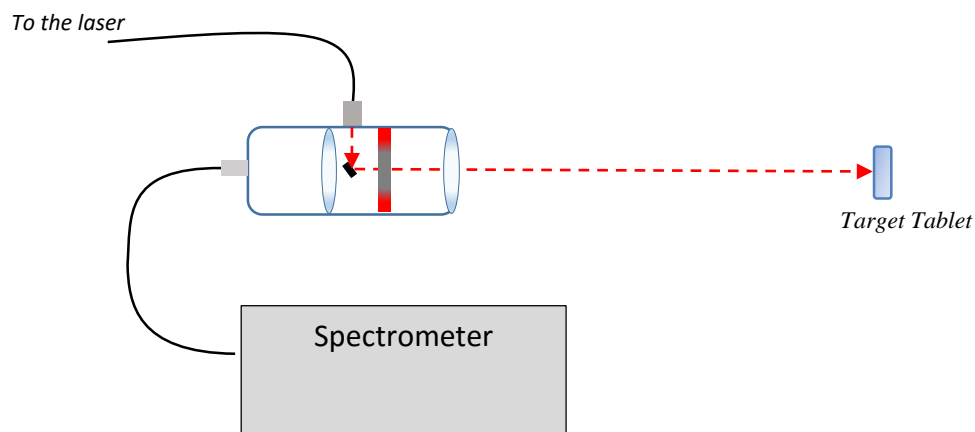


**Figure 10** Stand-off Raman setup

The target count levels were set to be 20000 to ensure the exposure times were similar to those used in the transmission setup. The resulting exposure required for the range of fibres is shown in Figure 11.

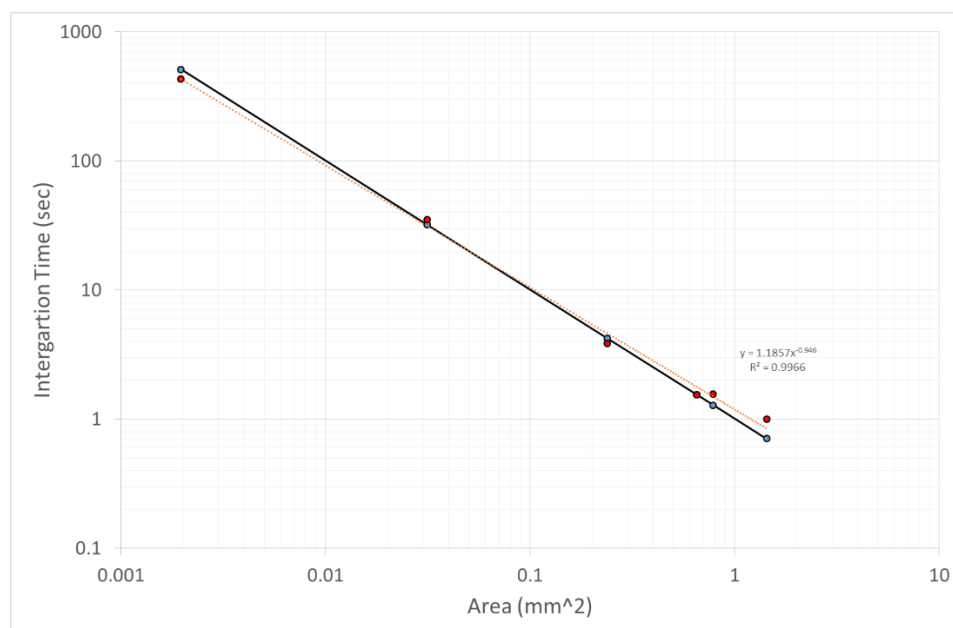


**Figure 11** Required integration time to observe 20000 counts per pixel as a function of fibre area when in a stand-off configuration (Red dots = observed data; Blue dots = simulated data)

As expected there is general good agreement between the experimental and theoretical results. However, the correlation is not as strong as that observed when operating in the transmission setup, the measured power coefficient across the range is -0.946. Once the fibre diameter exceeds 1 mm the gains observed are slightly lower than that expected from the area of the fibre. This is due to the nature of the scattering surface, and the profile of the light that strikes the tablet (which has a Gaussian intensity profile). In this standoff configuration the light is Lambertian scattered from

a diameter of  $\sim 1.5$  mm, this is lower than the 2.5 mm estimated by eye due to the intensity profile of the spot. Therefore the étendue of the target is comparable or slightly smaller than the spectrometer. This shows that in this type of measurement a standard HES spectrometer with a 1 mm fibre input would be acceptable for the target observation.

However, as the distance to the target increases it becomes difficult to maintain a small spot size. Given the signal strength is  $\propto 1/R^2$ , where R is the distance to the target, any loss of signal would be a concern.

### 5.1. Comparison with a dispersive spectrometer

The increased signal return in the standoff configuration allows the performance of a Czerny Turner spectrometer, which uses an uncooled CCD, to be examined and compared to HES 2003 instrument. The spectrometer has a slit of 0.2 mm  $\times$  1 mm. Figure 12 shows the resulting spectrum with an integration time of 1.55 seconds when the light is coupled to the system using the 0.91mm fibre. For comparison the return from the HES spectrometer is also shown, the data have been normalised for the display.

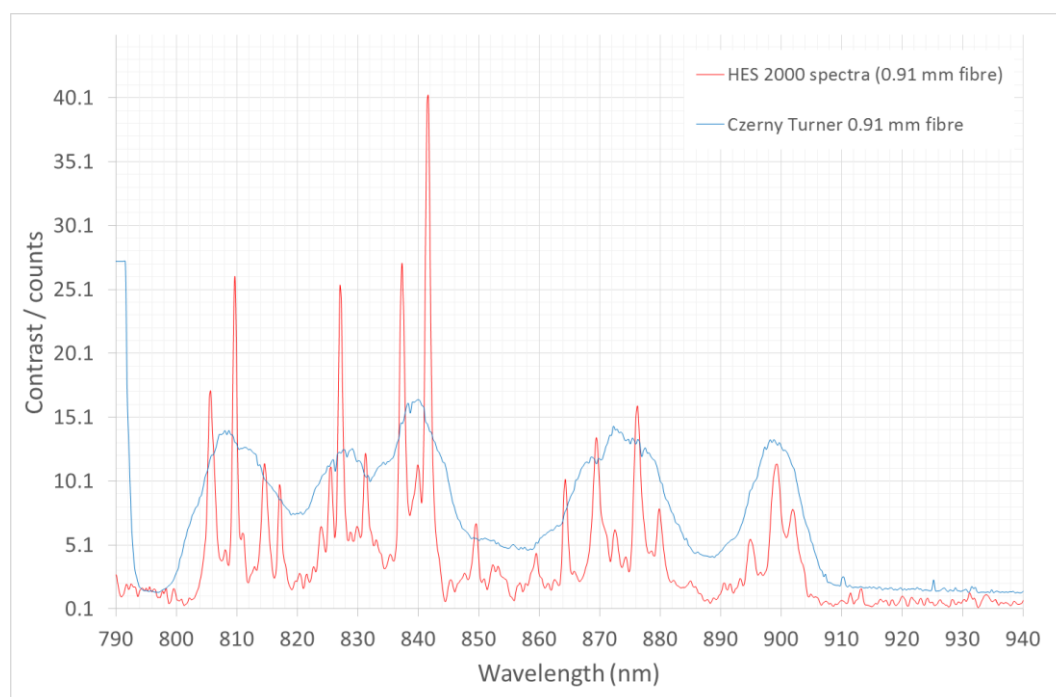


**Figure 12** Czerny turner return with 0.91 mm fibre, when operating in a stand off configuration (blue line), the equivalent HES 2003 response when using a 0.91 mm diameter fibre (red line).

Figure 12 shows that whilst the general shape of the paracetamol spectrum may be observed, the detailed information is lost due to the reduced resolution when operating with the 200  $\mu$ m slit. It should also be noted that the overall counts are lower than that observed by the HES system. To increase the resolution of the Czerny Turner instrument a 0.05 mm fibre was used. The resulting spectrum is shown in

Figure 13, overlaid with a corresponding HES measurement with a 50  $\mu\text{m}$  core fibre. When using the HES spectrometer the spectra become clear in  $\sim 10$  seconds, to achieve the 20000 counts per pixel 349 second was required.

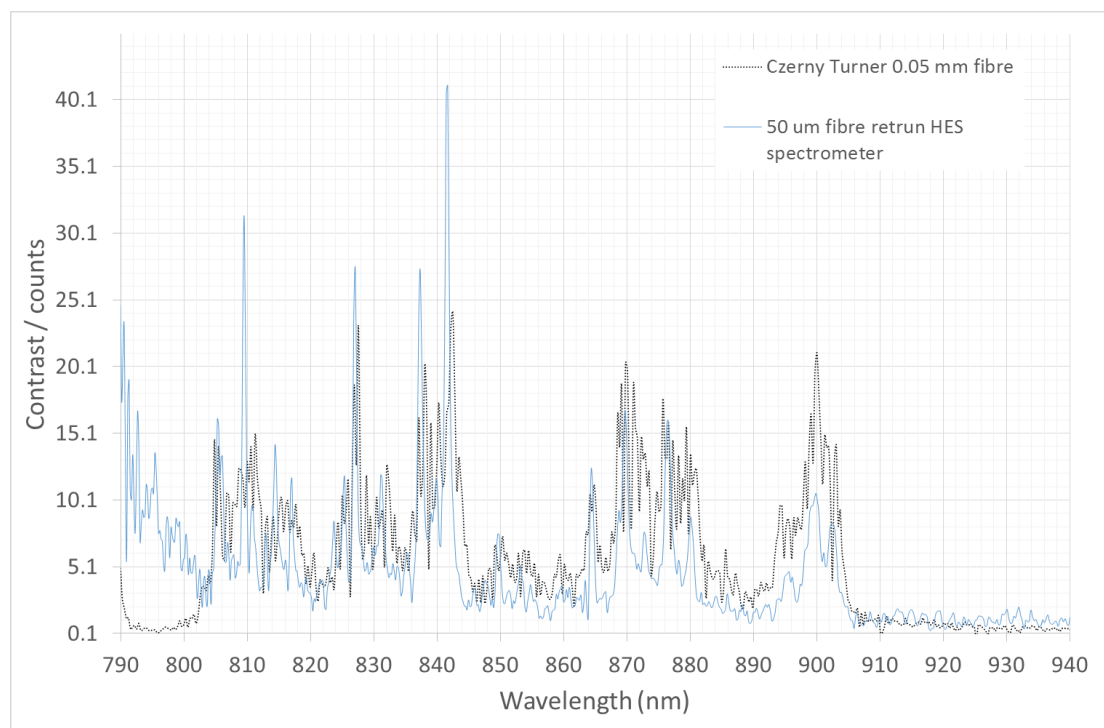


**Figure 13** Paracetamol spectra from stand-off configuration: Blue line = HES spectrometer return with 0.05 mm fibre; grey line = Czerny Turner return with 0.05 mm fibre.

Despite the resolution of the Czerny Turner being improved, the signal-to-noise is too low to resolve the feature clearly. The detector only allows for a maximum integration time of 20s limiting the amount of light that could be gathered.

## 6. Summary and Conclusions

The étendue advantage of static Fourier transform spectrometer has been experimentally demonstrated. In particular, the advantages of using this type of spectrometer design when performing transmission Raman observations has been shown through measurements made with a 3 mm diameter fibre bundle with no loss of resolution. To the knowledge of the Authors, this is a largest system of this type currently available, and represents a clear step forward for the technology.

The experiment has also demonstrated the homogenous nature of the light that exits a tablet when observed in transmission, demonstrating that Raman light comes from the bulk of the tablet volume, rather than a single spot on the surface.

The stand-off results show that similar gains are made when making observations in this configuration. However, if the full advantage of the system is to be realised it is important that the étendue of the target exceeds that of the instrument.

The demonstration shows that the HES range could provide key advantages in terms of speed of measurement or accuracy when making QA measurements in the pharmaceutical sector. It is ideal for making bulk measurements of samples (transmission Raman), and for stand-off observations when the target sample is difficult to reach. This could include applications with the process sector.

The total gains achieved by the instrument over a classical dispersive system when performing Transmission Raman results is > 500 in terms of throughput.

The HES2003 spectrometer is now available from IS-Instruments, for further information please visit our website:

[www.is-instruments.com](http://www.is-instruments.com) or contact us on [info@is-instruments.com](mailto:info@is-instruments.com)

## 7. References

- [AD1] Harlander. J., R. J Reynolds and F. L. Roesler., “ Spatial Heterodyne Spectrometer for the exploration of diffuse emission line a far ultraviolet wavelengths” *Astro Phys Journal* 396 (1992)
- [AD2] N. Overall, I. Priestnall., P. Dallin., J. Andrews., I. Lewis., K. Davis., H. Owen and M. W. George “ Measurement of spatial resolution and sensitivity in transmission and backscattering Raman spectroscopy of opaque samples: impact on pharmaceutical quality control and Raman tomography” *Applied Spectroscopy* (2010)
- [AD3] Czerny, M.; Turner, A. F. (1930). "Über den astigmatismus bei spiegelspektrometern.". *Zeitschrift für Physik* 61 (11–12): 792–797
- [AD4] <http://is-instruments.com/products.html>
- [AD5] Foster M. J., J Storey., P. Stockwell., and D Widdup, “ Stand off Raman spectrometer for identification of liquids in a pressurised gas pipeline” *Optics Express.*, Vol 23 Issue 3 (2015)